

# Cross-scale electric manipulations of cells and droplets by frequency-modulated dielectrophoresis and electrowetting†‡

Shih-Kang Fan,\* Po-Wen Huang, Tsu-Te Wang and Yu-Hao Peng

Received 25th February 2008, Accepted 23rd April 2008

First published as an Advance Article on the web 28th May 2008

DOI: 10.1039/b803204a

Two important electric forces, dielectrophoresis (DEP) and electrowetting-on-dielectric (EWOD), are demonstrated by dielectric-coated electrodes on a single chip to manipulate objects on different scales, which results in a dielectrophoretic concentrator in an EWOD-actuated droplet. By applying appropriate electric signals with different frequencies on identical electrodes, EWOD and DEP can be selectively generated on the proposed chip. At low frequencies, the applied voltage is consumed mostly in the dielectric layer and causes EWOD to pump liquid droplets on the millimetre scale. However, high frequency signals establish electric fields in the liquid and generate DEP forces to actuate cells or particles on the micrometre scale inside the droplet. For better performance of EWOD and DEP, square and strip electrodes are designed, respectively. Mammalian cells (Neuro-2a) and polystyrene beads are successfully actuated by a 2 MHz signal in a droplet by positive DEP and negative DEP, respectively. Droplet splitting is achieved by EWOD with a 1 kHz signal after moving cells or beads to one side of the droplet. Cell concentration, measured by a cell count chamber before and after experiments, increases 1.6 times from  $8.6 \times 10^5$  cells  $\text{ml}^{-1}$  to  $1.4 \times 10^6$  cells  $\text{ml}^{-1}$  with a single cycle of positive DEP attraction. By comparing the cutoff frequency of the voltage drop in the dielectric layer and the cross-over frequency of  $\text{Re}(f_{CM})$  of the suspended particles, we can estimate the frequency-modulated behaviors between EWOD, positive DEP, and negative DEP. A proposed weighted  $\text{Re}(f_{CM})$  facilitates analysis of the DEP phenomenon on dielectric-coated electrodes.

## Introduction

Regulating fluids and manipulating objects or particles of interest therein are two major tasks in most lab-on-a-chip (LOC) applications, especially when dealing with bio-fluids. First, it is because effective fluid regulation enables sample preparation, mixing, and transportation to a desired spot on a chip for further analyses. Thus, diverse micropumps, microvalves, and microchannels have hence been developed.<sup>1,2</sup> On the other hand, the ability to control a single or a group of particle(s) of interest in the fluid facilitates sample reaction, separation, and detection processes. Therefore, optical,<sup>3</sup> electric,<sup>4,5</sup> and magnetic<sup>6</sup> manipulations have been investigated to satisfy such a demand. In many cases, for the size differences, handling fluids and particles are regarded as two important but separate tasks, which are approached individually and independently by fundamentally different physical means. For instance, one may drive fluids through a piezoelectric mechanical micropump and move embedded particles with optical tweezers. In some applications,

however, instead of handling fluids and particles separately, it is helpful to achieve both tasks by related mechanisms in order to increase the portability and reduce the complexity of the LOC. Among all the manipulating mechanisms, the electric approach has been widely studied and successfully demonstrated to drive fluids and particles. For example, electrohydrodynamic<sup>7</sup> and electroosmotic<sup>8</sup> micropumps have been examined to regulate fluids in microchannels, while electrowetting-on-dielectric (EWOD)<sup>9</sup> has been applied in droplet-based digital microfluidics. In addition, electrophoresis<sup>4</sup> and dielectrophoresis (DEP)<sup>5</sup> are two phenomena that electrically manipulate charged and neutral particles electrically, respectively, in fluids. The above examples show that electric manipulation is cross-scale, which is desirable for driving objects on different scales.

Cho *et al.* first reported the manipulation of particles in a droplet by electrophoresis.<sup>10</sup> Concentration of the particles was achieved by splitting droplets using EWOD. Binary separation of carboxylate modified latex and polystyrene particles was further demonstrated. Recently, Cho *et al.* showed the concentration and separation of aldehyde sulfate latex particles or ground pine spores and glass beads by traveling-wave DEP (twDEP) for digital microfluidics.<sup>11</sup> In addition to electrical means, magnetic manipulations have also been investigated.<sup>12,13</sup> In most of the previous studies, droplet(s) was/were driven in the gap between parallel plates by EWOD electrodes; while particles were driven by additional electrodes or magnets. As a result, EWOD electrodes were placed on one plate, and electroporesis or twDEP electrodes for particles were fabricated on the other

Institute of Nanotechnology, National Chiao Tung University, 207R, Engineering Building 1, 1001 Ta Hsueh Road, Hsinchu, Taiwan.  
E-mail: skfan@mail.nctu.edu.tw; Fax: +886-3-5729912;  
Tel: +886-3-5712121 ext 55813

† The HTML version of this article has been enhanced with colour images.

‡ Electronic supplementary information (ESI) available: Derivations of curves in Fig. 6. Supplementary videos 1 and 2. See DOI: 10.1039/b803204a

plate of a parallel plate device. Here we show the integration of two intensively studied electric manipulations, EWOD and DEP, on dielectric-coated electrodes patterned on a single plate, to realize a cell (micrometre-sized) concentrator in a millimetre-sized droplet. By modulating the frequency of the applied AC signal on identical electrodes, droplet manipulation by EWOD and particle manipulation by DEP can be selectively achieved.

## Principle

### EWOD

EWOD is an electric means to change the wettability of a dielectric solid surface by applying a voltage across the dielectric layer. Sessile drop experiments are usually used to study this phenomenon by measuring the change in contact angle of a droplet on a dielectric-coated electrode caused by an applied voltage between the droplet and the underlying electrode.<sup>14</sup> With its ability to alter the contact angle of a droplet, EWOD has been applied in digital microfluidics and been developed as a driving force to create, transport, merge, and split droplets in parallel plate devices<sup>15,16</sup> (Fig. 1(a)). Such a device consists of a top plate, liquid droplet(s), and a bottom plate, denoted as A, B, and C in Fig. 1(a), respectively. The top plate contains a blank electrode covered by a hydrophobic Teflon layer. For observation purposes, an ITO glass is usually selected. An array of driving electrodes is patterned on the bottom plate and coated by a dielectric and a hydrophobic layer. The droplet is placed between top and bottom plates, with the height determined by the thickness of the spacers. When applying a voltage between the top and bottom plates, the surface above the energized

driving electrode is changed from hydrophobic to hydrophilic. Therefore, the droplet moves to the right as illustrated in Fig. 1(a). The contact angle change of the droplet on the energized driving electrode can be expressed by the Young–Lippmann equation:<sup>14,17</sup>

$$\cos\theta(V) = \cos\theta_0 + \frac{\epsilon_0 \epsilon_D}{2\gamma_{LG}t} V^2, \quad (1)$$

where  $\epsilon_0$  is the permittivity of vacuum,  $\epsilon_D$  and  $t$  are the relative permittivity and thickness of the dielectric layer, respectively, and  $\gamma_{LG}$  is the liquid–gas interfacial tension. When voltage  $V$  is applied across the dielectric layer, the contact angle changes from  $\theta_0$  to  $\theta(V)$ .

From eqn (1), the polarity and the frequency ( $f$ ) of the applied voltage appear not to alter the amount of contact angle change. However, it was found that EWOD is sensitive to the polarity for some dielectric materials. It was called asymmetric electrowetting and has been applied to drive and oscillate droplets.<sup>18</sup> In addition, the frequency also affects EWOD, or more precisely the voltage drop across the dielectric ( $V_D$ ), which can be analyzed by the simplified equivalent circuit of a droplet in a static situation as shown in Fig. 1(b). Similar electric models were reported and analyzed in the studies of EWOD and DEP liquid actuations.<sup>19,20</sup> When a direct current (DC) signal is applied, the entire applied voltage drops across the dielectric layer and causes EWOD ( $V_D = V$ ). When applying an alternating current (AC) signal, as the frequency of the signal increases,  $V_D$  decreases and the voltage drop across the liquid ( $V_L$ ) increases. At sufficiently high frequencies, the applied voltage drops entirely across the liquid ( $V_L = V$ ). Since the simplified equivalent circuit is composed of a resistor and capacitors, the time constant or the cutoff frequency ( $f_c$ ) provides general information about the frequency response of  $V_D$ .  $f_c$  can be expressed as:

$$f_c = \frac{1}{2\pi R_L(C_L + C_D)}, \quad (2)$$

Assuming the droplet is static and that it covers the whole surface of the energized driving electrode (Fig. 1(b)),  $R_L$ ,  $C_L$ , and  $C_D$  of eqn (2) can be substituted by the electric parameters of the liquid and dielectric layer:

$$f_c = \frac{\sigma_L}{2\pi\epsilon_0(\epsilon_L + \epsilon_D \frac{d}{t})}, \quad (3)$$

where  $\sigma_L$ ,  $\epsilon_L$ , and  $d$  are the conductivity, relative permittivity, and the height of the droplet, and  $\epsilon_D$  and  $t$  are the same relative permittivity and thickness of the dielectric layer as those in eqn (1). Based on eqn (3),  $f_c$  is varied by the combination of liquids and dielectric layers with different electrical properties and thicknesses in a parallel plate device. When applying an AC signal at  $f_c$ , there exists a voltage drop in the liquid ( $V_L \sim 0.37 V$ ) which decreases EWOD. In general, a DC signal drives droplets by EWOD most efficiently, but it is prone to electrolyze aqueous droplets and hinder their movements.<sup>21</sup> When the frequency of the applied signal is higher than  $f_c$ , e.g., hundreds of kHz for water droplets ( $f_c$  is on the order of a few kHz to tens of kHz), some other undesirable effects may occur, such as satellite droplet generation.<sup>22,23</sup> Therefore, driving droplets by EWOD

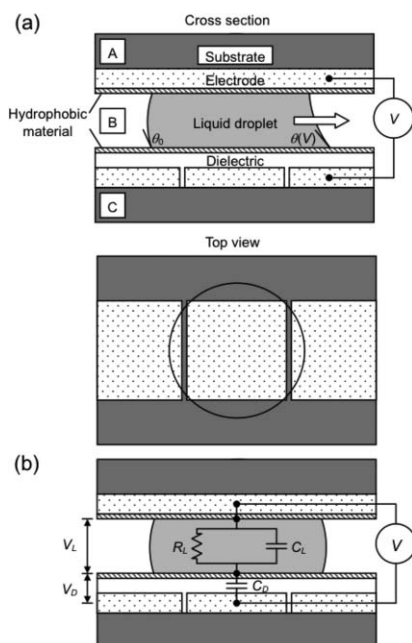


**Fig. 1** A parallel plate device to manipulate droplets by EWOD on an array of dielectric-covered driving electrodes. (a) Configuration of the device: A: top plate, B: liquid droplet, and C: bottom plate. (b) The simplified equivalent circuit of the device showing that the applied voltage would be distributed to  $V_D$  and/or  $V_L$  depending on the frequency.

by using an AC signal at a frequency below  $f_c$  (e.g., 1 kHz for water<sup>21,24</sup>) is commonly seen.

## DEP

Although a high frequency signal ( $f > f_c$ ) reduces or even causes EWOD to cease, it would establish an electric field in the droplet and become a driving force for the suspended particles therein. For example, a DC electric field could move charged particles suspended in a droplet by electrophoresis. However, to generate a DC electric field in a droplet, the dielectric layer of the parallel plate device should be removed or partially patterned.<sup>10</sup> In comparison to DC electric fields, AC electric fields in a droplet are more easily achieved without opening the dielectric layer by simply modulating the frequency of the applied voltage as described above. Depending on the frequency, the applied AC voltage  $V$  would partially or entirely contribute to the electric field in the droplet shown as  $V_L$  in Fig. 1(b). The frequency-dependent ratio of  $V_L/V$  can be expressed as:

$$V_L/V = \text{Re} \left\{ \frac{j2\pi f C_D R_L}{1 + j2\pi f (C_D + C_L) R_L} \right\} \quad (4)$$

$V_L$  in the droplet would further polarize the suspended neutral particles. If the electric field is non-uniform, polarized particles can be attracted to or repelled from high field strength regions by dielectrophoresis, or DEP.<sup>25–27</sup>

The force ( $F_{\text{DEP}}$ ) exerted on a spherical particle of radius  $a$  by DEP can be described by:<sup>25–27</sup>

$$F_{\text{DEP}} = 2\pi a^3 \epsilon_m \text{Re} \left\{ \frac{\epsilon_p^* - \epsilon_m^*}{\epsilon_p^* + 2\epsilon_m^*} \right\} \nabla E^2, \quad (5)$$

where  $E$  is the electric field,  $\epsilon_p^*$  and  $\epsilon_m^*$  are the complex permittivities of the manipulated particles and the suspension medium, respectively, which are frequency dependent and can be expressed as:<sup>25–27</sup>

$$\epsilon_{p,m}^* = \epsilon_0 \epsilon_{p,m} - j \frac{\sigma_{p,m}}{2\pi f}, \quad (6)$$

where  $\epsilon_{p,m}$  and  $\sigma_{p,m}$  are the relative permittivity and conductivity of the particle or the suspension medium, and  $f$  is the frequency of the field. From eqn (4) and (5), the magnitude and direction of  $F_{\text{DEP}}$  is found to be affected by  $f$ . To simplify further discussions, the frequency dependent term in eqn (5) is represented by the Clausius–Mossotti factor,  $f_{\text{CM}}$ .<sup>25–27</sup>

$$f_{\text{CM}} = \frac{\epsilon_p^* - \epsilon_m^*}{\epsilon_p^* + 2\epsilon_m^*}. \quad (7)$$

When the real part of  $f_{\text{CM}}$ , or  $\text{Re}(f_{\text{CM}})$ , is greater than zero,  $F_{\text{DEP}}$  attracts particles toward high field strength regions, which is referred to as positive DEP. On the contrary, a negative  $\text{Re}(f_{\text{CM}})$  generates negative DEP and repels particles from high field strength regions.

Since the gradient of the squared electric field magnitude ( $\nabla E^2$ ) plays a crucial role in  $F_{\text{DEP}}$ , manipulation of particles by DEP in a parallel plate device, as shown in Fig. 1, with both a high frequency ( $f > f_c$ ) signal and a redesigned electrode shape to create a non-uniform electric field is mandatory. Since the

EWOD force is proportional to the meniscus length overlapping with the energized electrode, square electrodes (Fig. 1) are usually designed with a comparable size as the droplet for a large and steady driving force. As a result, the electric field at high frequencies is almost uniform in a droplet as indicated by the electric field lines in Fig. 2(a). To create a non-uniform electric field inside a droplet in a dielectric-coated parallel plate device, shrunk electrodes (Fig. 2(b)) are as important as high frequency signals.

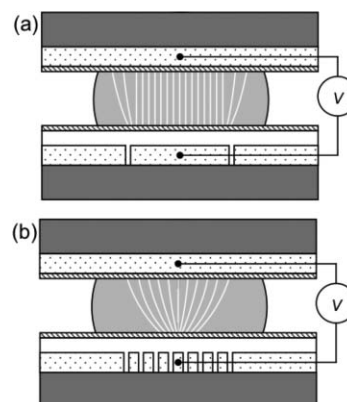


**Fig. 2** Electric field lines displaying the uniformity of the electric field in a droplet when applying a high frequency signal on the designed electrodes. (a) Square EWOD driving electrodes generate a nearly uniform electric field. (b) Shrunken electrodes establish a non-uniform electric field that is necessary for DEP actuations.

## Experimental

### Device design and fabrication

Our goal is to manipulate a droplet and suspended particles, including cells, on a single chip by electric manipulations: EWOD and DEP. To perform both EWOD and DEP effectively, two kinds of electrodes are designed as shown in Fig. 3(a). Eight strip electrodes ( $100 \mu\text{m} \times 1.6 \text{mm}$ ) in the center are mainly used to generate a non-uniform electric field in the droplet to actuate particles by DEP when applying high frequency signals, e.g., 2 MHz. Four square electrodes ( $1 \text{mm} \times 1 \text{mm}$ ) are designed to drive droplets by EWOD at low frequencies, e.g., 1 kHz. It is noteworthy that EWOD occurs when a 1 kHz signal is applied on the strip electrodes. Likewise, square electrodes can provide DEP if 2 MHz is applied. The applied frequency determines whether DEP or EWOD is generated; the shapes of the electrodes are designed for better performances of DEP or EWOD as discussed in the previous section. The reported manipulation mechanism emphasizes the frequency-modulated feature. This concept was first published in a conference proceeding,<sup>28</sup> which distinguishes itself from other digital microfluidic concentration or separation procedures introduced above.<sup>10–13</sup> The electrodes are patterned on the bottom plate of a parallel plate device and covered with dielectric and hydrophobic layers as shown in Fig. 3(b). The top plate contains a blank electrode coated with a thin hydrophobic layer. The gap between the plates is 200  $\mu\text{m}$ .

The procedure to concentrate the suspended particles in a liquid droplet is shown in Fig. 3(c)–(e). After a droplet is dispensed on top of the strip electrodes, the high frequency voltage (shown

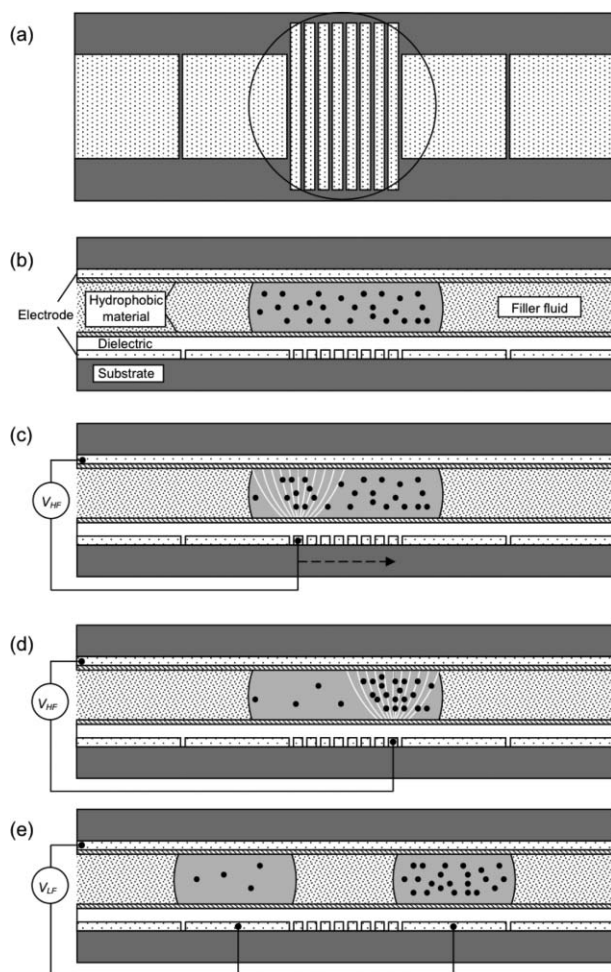


**Fig. 3** Configuration and driving procedure of a parallel plate device containing square and strip electrodes for droplets and suspended particle actuations by EWOD and DEP, respectively. (a) Top view. (b) Cross section. (c)–(d) By applying a high frequency signal ( $V_{HF}$ ) on one of the strip electrodes from left to right, the non-uniform electric field inside the droplet drives the particles to the right by DEP. (e) By applying a low frequency signal ( $V_{LF}$ ) on two of the square electrodes, two sub-droplets are obtained by EWOD with different particle concentrations.

$V_{HF}$  in Fig. 3) is applied on the very left strip electrode and switched from left (Fig. 3(c)) to right (Fig. 3(d)) sequentially. The energized strip electrodes generate non-uniform electric fields, causing particles driven by DEP from left to right. A similar particle/cell transportation was recently reported and named moving DEP (mDEP) by non-dielectric-covered electrodes in a microchannel.<sup>29</sup> After particles are moved to one side of the droplet (shown right side in Fig. 3(d)), the droplet is split into two sub-droplets with different particle concentrations by applying the low frequency voltage ( $V_{LF}$ ) as sketched in Fig. 3(e). Manipulated droplets are placed in an immiscible filler fluid of silicone oil to prevent evaporation, particle or protein adsorption,<sup>30,31</sup> and other undesirable phenomena such as satellite droplets at high frequencies.<sup>22,23</sup>

The tested devices are prepared by the following microfabrication steps. Au/Cr (450 Å/50 Å) electrodes are deposited and patterned as strip and square electrodes on the bottom plate. The bottom plate is then spun with 5 µm-thick SU-8 as a dielectric

layer and 500 Å-thick Teflon as a hydrophobic coating. The top plate has a blank ITO electrode coated with a hydrophobic layer (500 Å-thick Teflon). Before testing, a droplet is dispensed on the bottom plate and surrounded by the filler fluid, 50 cSt silicone oil. The top plate is then assembled onto the bottom plate with a 200 µm-high spacer in between.

### Cell concentration

Neuroblastoma cells (Neuro-2a) are prepared and tested in the concentration experiments. Neuro-2a cells are cultured in DMEM (Dulbecco's Modified Eagle's Medium), supplemented with 7.5% fetal bovine serum and 7.5% horse serum and incubated in 5% CO<sub>2</sub> at 37 °C. Prior to the experiments, cells are released from their flask by trypsin–EDTA. A suspension medium is prepared by adding 3% PBS in a 280 mM isotonic sucrose solution, resulting in a conductivity of 480 µS cm<sup>-1</sup>. The suspension medium is added to disperse centrifuged Neuro-2a cells for testing. The cell concentration measures 8.6 × 10<sup>5</sup> cells ml<sup>-1</sup> using a commercial cell count chamber (hemocytometer).

The experimental result of cell concentration is shown in Fig. 4. First, a 0.45 µl droplet containing Neuro-2a cells at the concentration of 8.6 × 10<sup>5</sup> cells ml<sup>-1</sup> is dispensed and immersed in the 50 cSt silicone oil filler fluid on the strip electrodes of the bottom plate. A top plate level with the bottom plate is carefully assembled to prevent capillary flow or droplet movement caused by the angle between the plates. After assembly, the parallel plates are spaced by a 200 µm-thick spacer. Before applying any voltage, the Neuro-2a cells, measuring 5 µm in diameter, are randomly dispersed in the droplets and are shown as the black dots in Fig. 4(a). Fig. 4(b)–(i) show the cells attracted by positive DEP when a 2 MHz and 60 V<sub>rms</sub> signal is applied on one of the strip electrodes from left to right. After the cells are concentrated to the right side in the droplet (Fig. 4(j)), the droplet is split into two sub-droplets by EWOD with 80 V<sub>rms</sub> and 1 kHz applied on the two adjacent square electrodes as shown in Fig. 4(k). By using a cell count chamber, we quantify the cell concentration of the right sub-droplet as 1.4 × 10<sup>6</sup> cells ml<sup>-1</sup>, while that of the left sub-droplet is 3.3 × 10<sup>5</sup> cells ml<sup>-1</sup>. As a result, by energizing the strip electrodes with a single cycle from left to right, the cells are concentrated 1.6 times (right sub-droplet) or diluted 2.6 times (left sub-droplet).

### Polystyrene bead concentration

Moreover, we investigate the concentration of polystyrene beads in the same parallel plate device with the same procedure. A 0.5 µl droplet containing 5 µm polystyrene beads at a concentration of 1.4 × 10<sup>8</sup> particles ml<sup>-1</sup> and surrounded by a 50 cSt silicone oil filler fluid is assembled in a parallel plate device as shown in Fig. 5(a). By sequentially applying a voltage (60 V<sub>rms</sub> and 2 MHz) on one of the strip electrodes from left to right, the polystyrene beads are repelled from left to right by negative DEP as shown in Fig. 5(b) and 5(d). Finally, most of the polystyrene beads are collected on the right side of the droplet (Fig. 5(e)). An 80 V<sub>rms</sub>, 1 kHz AC signal is then applied on the two square electrodes adjacent to the strip electrodes to split the original droplet into two sub-droplets. As shown in Fig. 5(f), two droplets with different polystyrene bead concentrations are obtained.

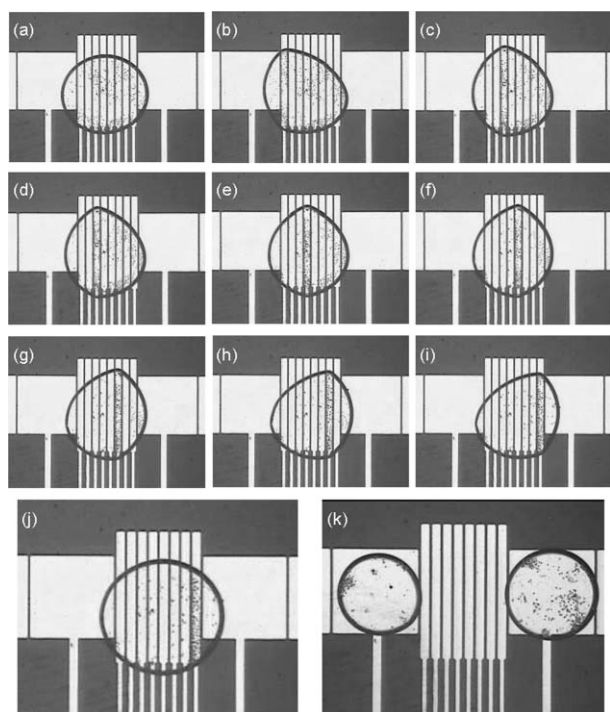


**Fig. 4** Mammalian cell (Neuro-2a) droplets concentrated by DEP and EWOD. (a) Cells are evenly suspended in a PBS and sucrose solution initially. (b)–(i) Cells are driven by positive DEP with a high frequency signal (2 MHz, 60 Vrms) sequentially applied to one of the eight strip electrodes from left to right. The images are taken when the driving voltage is applied. (j) Cells are concentrated on the right side of the droplet after DEP actuations (voltage is off). (k) Two sub-droplets of different cell concentrations are formed by applying a low frequency signal (1 kHz, 80 Vrms) to the two adjacent square electrodes. The supplementary video 1 can be seen in the ESI.†

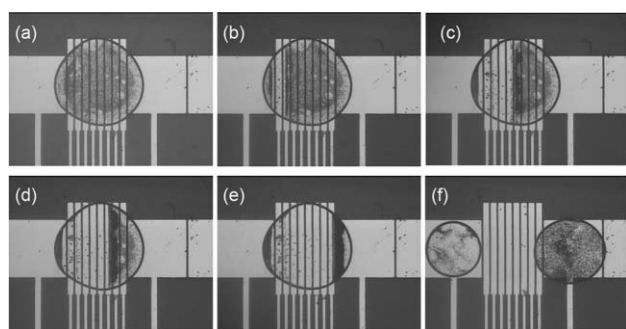


**Fig. 5** Polystyrene beads concentrated by DEP and EWOD. (a) Beads are evenly suspended in a water droplet initially. (b)–(e) Beads are driven by negative DEP (2 MHz, 60 Vrms) and concentrated on the right side of the droplet. (f) Droplet is split by EWOD (1 kHz, 80 Vrms). The supplementary video 2 can be seen in the ESI.†

## Discussions

### $\text{Re}(f_{\text{CM}})$ , $f_c$ , and $V_L/V$

The concentration of cells and polystyrene beads are successfully demonstrated by positive DEP and negative DEP, respectively, at 2 MHz. However, negative DEP actuation of cells or positive DEP actuation of polystyrene beads is not achieved in our available tested frequencies between DC and 2 MHz. In theory,

positive or negative DEP can be selectively obtained by altering the frequency of the applied field and estimated from the sign of  $\text{Re}(f_{\text{CM}})$  in eqn (7). Curve A in Fig. 6 shows  $\text{Re}(f_{\text{CM}})$  of Neuro-2a cells from 10 Hz to 1 GHz, which is calculated from a model of a spherical particle with a single shell.<sup>26,27</sup> The parameters used in the calculation are: 78, 10, and 60 as the relative permittivities ( $\epsilon$ ) of the suspension medium, cell membrane, and cytoplasm, respectively, and  $4.8 \times 10^{-2}$ ,  $1 \times 10^{-8}$ , and  $5 \times 10^{-1} \text{ S m}^{-1}$  as the conductivity ( $\sigma$ ) of the suspension medium, cell membrane, and cytoplasm, respectively. The diameter of the cell and the thickness of the cell membrane are 5  $\mu\text{m}$  and 5 nm, respectively. Most of the parameters follow the previous study<sup>26</sup> in addition to the measured conductivity of the suspension medium and the diameter of the cell. From curve A, it is confirmed that at 2 MHz the sign of  $\text{Re}(f_{\text{CM}})$  is positive, which is in accordance with the experimental results of positive DEP shown in Fig. 4. It appears that at low frequencies such as 1 kHz, the cells can be driven by negative DEP. However, from previous descriptions, a low frequency signal is consumed in the dielectric layer and generates little or no electric field in the droplet. It is now helpful to have  $f_c$  of  $V_D$ . By substituting  $4.8 \times 10^{-2} \text{ S m}^{-1}$  (medium), 78 (medium), 3 (SU-8), 200  $\mu\text{m}$  (medium), and 5  $\mu\text{m}$  (SU-8) for  $\sigma_L$ ,  $\epsilon_L$ ,  $\epsilon_D$ ,  $d$ , and  $t$  into eqn (3),  $f_c$  is calculated to be  $\sim 4.3 \text{ MHz}$ . Obviously, 1 kHz is too low to provide DEP actuations. Since 2 MHz is also below  $f_c$ , to estimate  $V_D$  and  $V_L$  at 2 MHz,  $V_L/V$  is plotted against

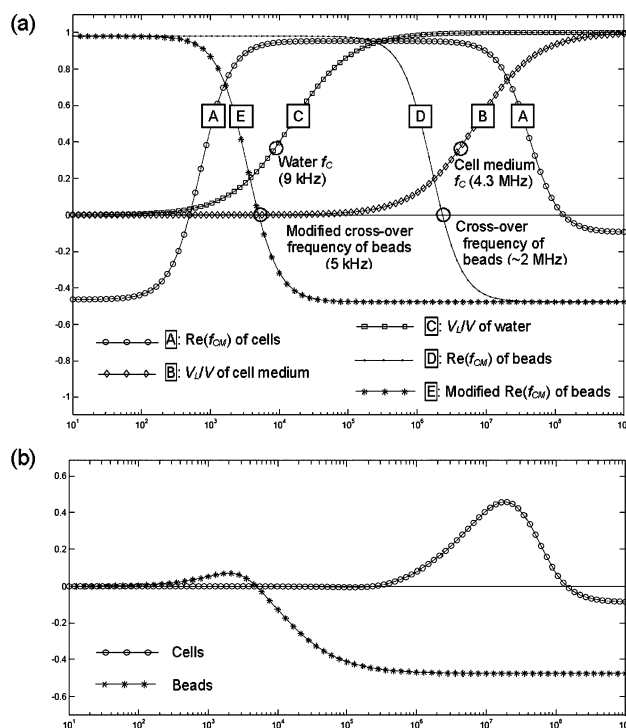


**Fig. 6** Frequency-dependant curves of the parallel plate device to analyze EWOD and DEP. (a)  $\text{Re}(f_{\text{CM}})$  of cells and beads, modified  $\text{Re}(f_{\text{CM}})$  of beads, and  $V_L/V$  of cells and bead show that positive DEP actuation of cells and negative DEP actuation of beads occur at 2 MHz. Low frequency signals would generate EWOD instead of negative DEP actuation of cells or positive DEP actuation of beads. (b) Weighted  $\text{Re}(f_{\text{CM}})$ , product of  $\text{Re}(f_{\text{CM}})$  and  $V_L/V$ , curves of cells and beads facilitate estimating DEP phenomena on dielectric-covered electrodes. The derivation of each curve is detailed in the supplementary material in the ESI.†

frequency (eqn (4)) as curve B in Fig. 6. At 2 MHz,  $\sim 20\%$  of the applied voltage  $V$  establishes the electric field in the droplet ( $V_L$ ), while the other  $\sim 80\%$  drops in the dielectric layer ( $V_D$ ). Since a large amount of  $V_D$  exists in the dielectric, when manipulating cells by DEP at 2 MHz, the EWOD effect can still be observed as the distortion of the droplet on the energized strip electrodes in Fig. 4 and the supplementary video 1 in the ESI.† To attract cells more effectively by positive DEP, one can apply a signal of a higher frequency or decrease the conductivity of the medium to reduce  $f_C$  and increase  $V_L$  at 2 MHz, as indicated by curve C in Fig. 6.

Curve C in Fig. 6 displays  $V_L/V$  of water ( $\sigma_L = 1 \times 10^{-4} \text{ S m}^{-1}$ ,  $\epsilon_L = 80$ ), which possesses a much lower  $f_C$  at  $\sim 9 \text{ kHz}$ . Therefore, in the case of polystyrene bead actuation, 2 MHz is sufficiently high to eliminate EWOD since  $V_L/V$  is close to 1. It is confirmed from Fig. 5 and the supplementary video 2 in the ESI‡ that the droplet is not altered or deformed when applying a 2 MHz signal to drive polystyrene beads.  $\text{Re}(f_{\text{CM}})$  of polystyrene beads is also plotted as curve D in Fig. 6 by substituting 2.5 for  $\epsilon_p$ ,  $1 \times 10^{-2}$  for  $\sigma_p$ ,<sup>26</sup> and the corresponding parameters of water into eqn (6) and (7). The curve shows that the value of  $\text{Re}(f_{\text{CM}})$  is changed from positive to negative at  $\sim 2 \text{ MHz}$ , which is also called the cross-over frequency. In theory, the polystyrene beads should be slightly polarized, and the DEP is negligible at 2 MHz. However, our experimental results show noticeable negative DEP at 2 MHz, meaning that the cross-over frequency is below 2 MHz. It was reported that the cross-over frequency is sensitive to the size of the beads.<sup>32</sup> Instead of 2 MHz, the cross-over frequency of  $5 \mu\text{m}$  polystyrene beads was found to be  $\sim 5 \text{ kHz}$ . Although it may not represent the real condition, for easier analyses we shift the  $\text{Re}(f_{\text{CM}})$  (curve D) so that the cross-over frequency is at 5 kHz (curve E) as shown in Fig. 6. From the  $V_L/V$  curve of water (curve C) and the modified  $\text{Re}(f_{\text{CM}})$  curve of polystyrene beads (curve E), we realize that positive DEP of polystyrene beads is not possible for the tested dielectric-covered electrodes.

### Weighted $\text{Re}(f_{\text{CM}})$

With the same electrode design and fixed magnitude of the applied signal, *i.e.*,  $\nabla E^2$  is a constant, frequency-dependent  $F_{\text{DEP}}$  can be predicted by  $\text{Re}(f_{\text{CM}})$ . For example, one may not utilize a signal at the cross-over frequency because  $\text{Re}(f_{\text{CM}})$  is zero and  $F_{\text{DEP}}$  is negligible. However, the prediction of  $F_{\text{DEP}}$  by  $\text{Re}(f_{\text{CM}})$  is not satisfactory for electrodes covered by a dielectric layer as described in this paper since the  $V_L/V$  ratio is also varied by frequency, *i.e.*,  $\nabla E^2$  is no longer a constant to varied frequencies. As discussed above, negative DEP of cells are not achieved because no electric field is established in the droplet at low frequencies. In other words, because curve B ( $V_L/V$ ) in Fig. 6(a) is approximately zero at low frequencies,  $\nabla E^2$  is insignificant. Therefore, we propose a weighted  $\text{Re}(f_{\text{CM}})$ , which is the product of  $V_L/V$  and  $\text{Re}(f_{\text{CM}})$ , to better estimate DEP on dielectric-coated electrodes as shown in Fig. 6(b). For example, the weighted  $\text{Re}(f_{\text{CM}})$  curve of the cells is obtained from curve A and B of Fig. 6(a). The weighted  $\text{Re}(f_{\text{CM}})$  curves clearly explain that cells would only be driven by positive DEP in the tested frequencies (DC to 2 MHz), while negative DEP actuation of beads is achieved in most of the tested frequencies. Although

positive DEP of beads may occur at  $\sim 2 \text{ kHz}$ ,  $F_{\text{DEP}}$  is too small to be observed in the experiment for the limited weighted  $\text{Re}(f_{\text{CM}})$  and significant EWOD at low frequencies. From Fig. 6(b), the optimum frequency for positive DEP of cells would be at  $\sim 20 \text{ MHz}$ . To analyze  $F_{\text{DEP}}$  on dielectric-covered electrodes, one should substitute the weighted  $\text{Re}(f_{\text{CM}})$  for  $\text{Re}(f_{\text{CM}})$  in eqn (5) and recalculate  $\nabla E^2$  caused by  $V_L$  from eqn (4).

### Concentration parameters

In our experiment, the DEP signal (2 MHz, 60 Vrms) is applied on each strip electrode until most of the particles on the adjacent electrodes are attracted or repelled by DEP. From supplementary video 1 and 2 in the ESI,‡ the cells are attracted in 30 s, and the beads are repelled in 10 s. It is because the weighed  $\text{Re}(f_{\text{CM}})$  of cells is smaller than that of the beads at 2 MHz. The frequency and amplitude of the DEP signal (2 MHz, 60 Vrms) are limited by our apparatus. Although the results are not shown, a lower voltage slows the concentration. By using a higher voltage, a faster separation is expected. However, the risk of damaging the cells would become higher. In the case of cell concentration, to lower the applied voltage while maintaining the concentration speed or to increase the throughput with the same voltage, one could shorten the width of the strip electrodes to increase  $\nabla E^2$ , or increase the frequency, *e.g.*, 20 MHz, to obtain a higher weighted  $\text{Re}(f_{\text{CM}})$ .

Cell viability is monitored by observing cell conformation during the experiment and staining cells with Trypan blue after the experiment. Since the cells start to lose their viability in the isotonic suspension medium for more than one hour, experiments are performed right after the cells are released from the flask and finished within one hour. During the experiment, changing of cell conformation and cell lysis are not observed, as shown in Fig. 4 and supplementary video 1 in the ESI.‡ After the experiment, the cells are almost not stained by Trypan blue, meaning the cells are still viable. In comparison with other experiments of cell DEP, the applied voltage (2 MHz, 60 Vrms) appears to be large. However, from the previous analysis of  $V_L/V$ , the real voltage applied in the droplet ( $V_L$ ) causing DEP is 12 Vrms (*i.e.*, 0.2 V), resulting in a  $6 \times 10^4 \text{ V m}^{-1}$  electric field, which is similar to other DEP experiments. Gary *et al.*<sup>33</sup> found the viability of BPAECs cells that underwent a 2 MHz,  $6.25 \times 10^4 \text{ V m}^{-1}$  for 30 min was close to 100%. The morphologies of the DEP cells were similar to controls over 2 days in culture. Cell viability studies with comparable electric field strengths suggested that the field has no appreciable effects on the cells.<sup>34–37</sup>

It is observed that the movements of the particles during DEP concentrations are localized. As shown in Fig. 4, the cells on the electrodes adjacent to the energized electrode can be attracted; while the rest of the cells keep stationary. It implies that the initial dispersion of the cells has limited effect on the results. Furthermore, the concentration ability is expected to increase by multiple cycle actuations. The cell concentration can be increased twice at most under current procedures because two sub-droplets are split. To increase the concentration, more droplets or smaller droplets need to be split at the last step.

Finally, the possibility of binary separation, an interesting function in digital microfluidics to drive two types of particles in opposite directions and confine them in different

sub-droplets,<sup>10,11</sup> is discussed. Although it has not been experimentally confirmed, binary separation is feasible in the proposed device by sweeping an appropriate signal on the strip electrodes back and forth at least once. Assuming that the signal attracts A particles by positive DEP and repels B particles by negative DEP, by sweeping the signal from left to right, A particles would be attracted to the very right strip electrode, while B particles would be repelled farther beyond it. As the signal is swept back from right to left, A particles are expected to be driven to the left, while B particles stay at the right. The subsequent droplet splitting should achieve the binary separation function. Carefully choosing the separation parameters for A and B particles possessing similar weighted  $\text{Re}(f_{\text{CM}})$  increases the separation efficiency. The cell fractionation<sup>29</sup> of viable and nonviable yeast cells in a microchannel demonstrated by mDEP is an interesting study close to the binary separation in a droplet.

## Conclusions

Two cross-scale electric manipulations, EWOD and DEP, are successfully demonstrated by modulating the frequency of the applied signal in a parallel plate device with dielectric-coated electrodes. At low frequencies (e.g., 1 kHz), the applied signal mainly exists in the dielectric layer and causes EWOD to drive droplets on the mm scale. At high frequencies (e.g., 2 MHz), the applied signal establishes a non-uniform electric field in the droplet and generates DEP forces exerting on the suspended particles including mammalian cells and polystyrene beads. Cell and bead concentrations are achieved by DEP and EWOD. Frequency-dependent  $V_L/V$  and  $f_C$  are calculated from the simplified equivalent circuit of the device to realize the voltage distributions in dielectric ( $V_D$ ) and liquid ( $V_L$ ).  $\text{Re}(f_{\text{CM}})$  and  $V_L/V$  are plotted to estimate DEP actuation of cells and beads. The weighted  $\text{Re}(f_{\text{CM}})$  is proposed for DEP force predictions on dielectric-coated electrodes.

## Acknowledgements

This work is partially supported by the National Science Council, Taiwan, R.O.C. under grants NSC 95-2221-E-009-266-MY3, NSC 96-2627-M-009-001, and NSC 96-2218-E-006-294.

## References

- 1 G. M. Whitesides, *Nature*, 2006, **442**, 368–373.
- 2 D. J. Laser and J. G. Santiago, *J. Micromech. Microeng.*, 2004, **14**, R35–R64.
- 3 D. G. Grier, *Nature*, 2003, **424**, 810–816.
- 4 G. J. M. Bruin, *Electrophoresis*, 2000, **21**, 3931–3951.
- 5 P. R. C. Gascoyne and J. Vykoukal, *Electrophoresis*, 2002, **23**, 1973–1983.
- 6 H. Lee, A. M. Purdon and R. M. Westervelt, *Appl. Phys. Lett.*, 2004, **85**, 1063–1065.
- 7 G. Fuhr, T. Schnelle and B. Wagner, *J. Micromech. Microeng.*, 1994, **4**, 217–226.
- 8 R. B. M. Schasfoort, S. Schlautmann, J. Hendrikse and A. Van Den Berg, *Science*, 1999, **286**, 942–945.
- 9 F. Mugele and J.-C. Baret, *J. Phys.: Condens. Matter*, 2005, **17**, R705–R774.
- 10 S. K. Cho, Y. Zhao and C.-J. Kim, *Lab Chip*, 2007, **7**, 490–498.
- 11 Y. Zhao, U.-C. Yi and S. K. Cho, *J. Microelectromech. Syst.*, 2007, **16**, 1472–1481.
- 12 Y. Wang, Y. Zhao and S. K. Cho, *J. Micromech. Microeng.*, 2007, **17**, 2148–2156.
- 13 U. Lehmann, S. Hadjidj, V. K. Parashar, C. Vandevyver, A. Rida and M. A. M. Gijs, *Sens. Actuators, B*, 2006, **117**, 457–463.
- 14 B. Berge, *C. R. Acad. Sci.*, 1993, **II 317**, 157–163.
- 15 M. G. Pollack, R. B. Fair and A. D. Shenderov, *Appl. Phys. Lett.*, 2000, **77**, 1725–1726.
- 16 S. K. Cho, H. Moon and C.-J. Kim, *J. Microelectromech. Syst.*, 2003, **12**, 70–80.
- 17 M. Vallet, B. Berge and L. Bovellet, *Polymer*, 1996, **37**, 2465–2470.
- 18 S.-K. Fan, H. Yang, T.-T. Wang and W. Hsu, *Lab Chip*, 2007, **7**, 1330–1335.
- 19 T. B. Jones, M. Gunji, M. Washizu and M. J. Feldman, *J. Appl. Phys.*, 2001, **89**, 1441–1448.
- 20 T. B. Jones, J. D. Fowler, Y. S. Chang and C.-J. Kim, *Langmuir*, 2003, **19**, 7646–7651.
- 21 S.-K. Fan, Ph.D. Thesis, University of California, Los Angeles, 2003.
- 22 M. Vallet, M. Ballade and B. Berge, *Eur. Phys. J. B*, 1999, **11**, 583–591.
- 23 F. Mugele and S. Herminghaus, *Appl. Phys. Lett.*, 2002, **81**, 2303–2305.
- 24 S. K. Cho, S.-K. Fan, H. Moon and C.-J. Kim, *Proc. IEEE Conf. MEMS*, 2002, 32–35.
- 25 H. A. Pohl, *Dielectrophoresis*, Cambridge University Press, Cambridge, 1978.
- 26 H. Morgan and N. G. Green, *AC Electrokinetics: colloids and nanoparticles*, Research Studies Press Ltd., Baldock, 2003.
- 27 T. B. Jones, *Electromechanics of Particles*, Cambridge University Press, Cambridge, 1995.
- 28 P.-W. Huang, T.-T. Wang, S.-W. Lin, Y.-C. Chang and S.-K. Fan, *Proc. IEEE Conf. NEMS*, 2006, 1418–1421.
- 29 C. H. Kua, Y. C. Lam, I. Rodriguez, C. Yang and K. Youcef-Toumi, *Anal. Chem.*, 2007, **79**, 6975–6987.
- 30 J.-Y. Yoon and R. L. Garrell, *Anal. Chem.*, 2003, **75**, 5097–5102.
- 31 V. Srinivasan, V. K. Pamula and R. B. Fair, *Lab Chip*, 2004, **4**, 310–315.
- 32 J. Auerswald and H. F. Knapp, *Microelectron. Eng.*, 2003, **67–68**, 879–886.
- 33 D. S. Gary, J. L. Tan, J. Voldman and C. S. Chen, *Biosens. Bioelectron.*, 2004, **19**, 771–780.
- 34 H. Glasser and G. Fuhr, *Bioelectrochem. Bioenerg.*, 1998, **47**, 301–310.
- 35 S. Archer, T.-T. Li, A. T. Evans, S. T. Britland and H. Morgan, *Biochem. Biophys. Res. Commun.*, 1999, **257**, 687–689.
- 36 T. Heida, P. Vulto, W. L. C. Rutten and E. Marani, *J. Neurosci. Methods*, 2001, **110**, 37–44.
- 37 A. Docoslis, N. Kalogerakis and L. A. Behie, *Cytotechnology*, 1999, **30**, 133–142.